

See discussions, stats, and author profiles for this publication at: <https://www.researchgate.net/publication/259447251>

Assessment of land surface temperature and heat fluxes over Delhi using remote sensing data

Article in *Journal of Environmental Management* · December 2013

DOI: 10.1016/j.jenvman.2013.11.034 · Source: PubMed

CITATIONS

139

READS

1,381

3 authors:



Surya Deb Chakraborty

Environmental Systems Research Institute (ESRI)

12 PUBLICATIONS 173 CITATIONS

SEE PROFILE



Yogesh Kant

Indian Space Research Organization

90 PUBLICATIONS 1,928 CITATIONS

SEE PROFILE



Debashis Mitra

Indian Institute of Remote Sensing, Indian Space Research Organization

133 PUBLICATIONS 2,588 CITATIONS

SEE PROFILE



Contents lists available at ScienceDirect

Journal of Environmental Management

journal homepage: www.elsevier.com/locate/jenvman

Assessment of land surface temperature and heat fluxes over Delhi using remote sensing data

Surya Deb Chakraborty^a, Yogesh Kant^{b,*}, Debashis Mitra^b

^aIndian Institute of Science, Bengaluru, India

^bIndian Institute of Remote Sensing, ISRO, Dehradun, India

ARTICLE INFO

Article history:

Received 8 July 2013

Received in revised form

27 October 2013

Accepted 22 November 2013

Available online xxx

Keywords:

Land surface temperature

Emissivity

LU/LC change

Sensible heat flux

Latent heat flux

Anthropogenic heat flux

ABSTRACT

Surface energy processes has an essential role in urban weather, climate and hydrosphere cycles, as well in urban heat redistribution. The research was undertaken to analyze the potential of Landsat and MODIS data in retrieving biophysical parameters in estimating land surface temperature & heat fluxes diurnally in summer and winter seasons of years 2000 and 2010 and understanding its effect on anthropogenic heat disturbance over Delhi and surrounding region. Results show that during years 2000–2010, settlement and industrial area increased from 5.66 to 11.74% and 4.92 to 11.87% respectively which in turn has direct effect on land surface temperature (LST) and heat fluxes including anthropogenic heat flux. Based on the energy balance model for land surface, a method to estimate the increase in anthropogenic heat flux (H_{as}) has been proposed. The settlement and industrial areas has higher amounts of energy consumed and has high values of H_{as} in all seasons. The comparison of satellite derived LST with that of field measured values show that Landsat estimated values are in close agreement within error of $\pm 2^\circ\text{C}$ than MODIS with an error of $\pm 3^\circ\text{C}$. It was observed that, during 2000 and 2010, the average change in surface temperature using Landsat over settlement & industrial areas of both seasons is 1.4°C & for MODIS data is 3.7°C . The seasonal average change in anthropogenic heat flux (H_{as}) estimated using Landsat & MODIS is up by around 38 W/m^2 and 62 W/m^2 respectively while higher change is observed over settlement and concrete structures. The study reveals that the dynamic range of H_{as} values has increased in the 10 year period due to the strong anthropogenic influence over the area. The study showed that anthropogenic heat flux is an indicator of the strength of urban heat island effect, and can be used to quantify the magnitude of the urban heat island effect.

© 2013 Published by Elsevier Ltd.

1. Introduction

The fast expansion of urban area results in change of local atmosphere and surface temperature compared to the surrounding rural area. The temperature gradient represents human-urban and rural contrast, which is due to deforestation and the replacement of the land surface by non-evaporating and nonporous materials such as asphalt and concrete. This results in reduced evapotranspiration and more rapid runoff of rain water (Carlson, 1986). The thermal behavior and characteristics of urban surface is an important data for urban planners and architects for improving city site quality making more eco-friendly. Land surface temperature (LST) and emissivity are important parameters in energy budget estimation, land cover assessment and other earth surface characteristic related

studies (Srivastava et al. 2010; Chang et al. 2010). Study of the heat island requires understanding the role of land surface parameter, evapotranspiration, surface heat fluxes and the overall influence of urban features on thermal environment (Dousset and Gourmelon 2003; Boegh and Soegaard, 2004). Remote sensing can provide information on parameters such as surface albedo, vegetation index, surface emissivity and surface temperature that are inputs for estimating surface heat fluxes which are otherwise difficult in obtaining the spatial and temporal information from traditional ground based *in situ* measurements. The urban heat-island effect occurs as a result of increased sensible heat flux from the land surface to the atmosphere near cities. Sensible heat flux consists of two components, heat radiation due to solar input and heat due to anthropogenic discharge. The latter may be enhanced by changes in the usage of artificial land surface (Soushi and Yasushi, 2005). The present work follows a new method to separate the anthropogenically discharged heat and natural heat radiation from the sensible heat flux based on a heat-balance model using satellite remote

* Corresponding author.

E-mail address: ykant@yahoo.com (Y. Kant).

sensing and ground meteorological data. Anthropogenic heat discharge in all the seasons in the area is found to be around 94 W/m² on an average, namely more than 18% of natural sensible heat flux. The objective of the study was to analyze the potential of Landsat and MODIS data in estimating surface emissivity and LST. The surface heat fluxes (including natural & anthropogenic) were quantitatively estimated over various LU/LC features using Landsat and MODIS data. Spatial and seasonal variation of heat fluxes were evaluated and compared for summer and winter seasons of year 2000 and 2010 and its effect on anthropogenic heat distribution over Delhi and surrounding areas. Net radiation was estimated from albedo, surface emissivity, surface and atmospheric temperature and solar radiation. Sensible and latent heat fluxes were estimated via the bulk resistance approach using surface and atmospheric temperature, wind speed and relative humidity.

2. Study area

The study was carried out over Delhi and surrounding areas situated between latitude 28°14'57" N to 28°52'18" N and longitude between 77°35'34" E to 76°57'38" E and altitude lies between 213 and 305 m covering an area of 5160.00 km². Delhi climatic type is a monsoon-influenced humid subtropical (Köppen climate classification Cwa). One of the most characteristic features of Delhi climate is extreme low and high temperature ranging to as high as 47 °C during summer while reaching as low as -0.6 °C during winter (Source IMD). January being the coldest, May/June the hottest and mean annual total rainfall is around 70 cm. Physically Delhi can be divided into three segments: the Yamuna flood plain, the ridge and the plain. The Yamuna flood plain is somewhere low-lying and sandy. The ridge constitutes the most dominating physiographic features of this territory. It originates from the Aravali hills of Rajasthan and enter Delhi from the south, extends in north-eastern direction and the rest of Delhi is categorized as a plain. Yamuna is the main river that passes through Delhi. Apart from the flood channels of Yamuna there are 3 canals, i.e. portion of Agra Canal, Hindu Canal and western Yamuna canal. The vegetation in the ridge (forest) is predominately of thorny scrub type, which is usually found in arid and semi-arid zone. Ridge Forest of Delhi falls in the category of 'Tropical thorn forest' as per the forest type classification of Champion and Seth (1968), and more especially as 'semi-arid open scrub' and among trees that are dominant is Acacias.

3. Data and material

The seasonal & diurnal heat fluxes were estimated using Landsat TM-5 and MODIS datasets over different Land use (LU)/Land Cover (LC) of Delhi area over 10 year of time period. Landsat TM-5 data is used for preparation of land use/land cover maps and estimation of surface temperature and heat fluxes.

All the satellite images were geometrically rectified and atmospheric FLAASH correction was applied in all datasets of Landsat and MODIS (Table 1). The land use/land cover classifications were performed using Landsat image of February 2000 and 2010

datasets. Eventually, the land surface was classified into eight types of land cover classes: agriculture, settlement, water body, Open scrub, Open space with grass, Forest, Bare soil and Industries. The datasets were used to retrieve biophysical parameters like NDVI, albedo and surface emissivity to estimate surface temperature, net radiation and sensible heat flux.

4. Methodology

Heat fluxes was estimation over various land use/land cover on several days of winter (February) and summer (May) seasons of year 2000 and 2011. After applying the geometric correction, the subset images of radiance were created both for visible and near infrared bands of Landsat TM-5 and MODIS datasets. For effective estimation of temperature, the surface emissivity values are to be derived at pixel level (Kant and Badarinath, 2002). It is found that the emissivity over vegetation in 8–14 μm region remains more or less uniform (Nichol, 1995). The proportion of vegetation cover in conjunction with NDVI was taken to estimate pixel emissivity (Grind and Owe, 1993).

$$\epsilon = a + b \cdot \ln(\text{NDVI}) \quad (1)$$

where $a = 1.0094$ and $b = 0.047$ where, $\text{NDVI} = \frac{\rho_{\text{NIR}} - \rho_{\text{Red}}}{(\rho_{\text{NIR}} + \rho_{\text{Red}})}$ ρ = Reflectance

Landsat-TM band 6 imagery was converted from spectral radiance (as described above) to a more physically useful variable (NASA, 2004). This is the effective at-satellite temperatures of the viewed Earth-atmosphere system under an assumption of unity emissivity and using pre-launch calibration constants (Mansor and Cracknell, 1994). The digital number (DN) of thermal infrared band is converted in to spectral radiance (L_λ) using the calibration constants and incorporation of surface emissivity estimates the surface temperature as,

$$T = \frac{K_2}{\ln\left(\frac{\epsilon K_1}{L_\lambda}\right) + 1} \quad (2)$$

where $K_1 = 607.76 \text{ mWcm}^{-2} \text{ sr}^{-1} \mu\text{m}^{-1}$, $K_2 = 1260.56 \text{ K}$, L_λ = radiance, ϵ = emissivity

The split window used for MODIS was developed by Wan and Dozier (1996), and is defined as.

$$T_s = c + \left(A_1 + A_2 \frac{1 - \epsilon}{\epsilon} + A_3 \frac{\Delta\epsilon}{\epsilon^2} \right) \frac{T_{31} - T_{32}}{2} + \left(B_1 + B_2 \frac{1 - \epsilon}{\epsilon} + B_3 \frac{\Delta\epsilon}{\epsilon^2} \right) \frac{T_{31} - T_{32}}{2} \quad (3)$$

$$\epsilon = (\epsilon_{31} + \epsilon_{32})/2$$

$$\Delta\epsilon = \epsilon_{31} - \epsilon_{32}$$

The narrow band emissivities can be obtained from the broad band values using the relation (Rubio et al., 1997),

$$\epsilon_i = A \epsilon_{8-14} + B \quad (4)$$

$i = 31, 32$ band, A & B are coefficients (Rubio et al. 1997) where T_{31} and T_{32} are the brightness temperatures measured for MODIS bands 31 and 32, respectively; ϵ_{31} & ϵ_{32} are MODIS band 31 and 32 surface emissivity; and $A_1, A_2, A_3, B_1, B_2, B_3$ and C are regression coefficients. These coefficients are available during algorithm execution via a look up table (LUT) based on the results of radiative transfer simulation under a large range of surface & atmospheric conditions are derived using linear regression.

Table 1

The following datasets were used to compute seasonal and temporal LST and heat fluxes.

Dataset used	Summer		Winter	
	Year (2000)	Year (2010)	Year (2000)	Year (2010)
Landsat TM-5	May 9	May 5	February 3	February 14
MODIS level 1B data	May 10	May 22	February 28	February 26

For natural land surface the energy balance is described as,

$$R_n = LE + G + H \quad (5)$$

where R_n is net radiation, G is the ground heat flux, LE is the latent heat flux, H is sensible heat flux. Latent heat is created by evapotranspiration of land surfaces while the sensible heat is transferred from land surface to atmosphere.

Over urban areas in addition to the net radiation, the anthropogenic heat discharge mainly from urban structures and transportation also adds to the heat fluxes component. The heat balance equation is described as,

$$R_n + A = LE + G + H \quad (6)$$

where A is the total anthropogenic heat discharge.

The incoming components are positive and outgoing is counted as negative. The net radiation is the sum of the incoming and outgoing short and long wave components. Net radiation R_n is the dominant term in the Energy Balance Equation (EBE), since it represents the source of energy that must be balanced by the thermodynamic equilibrium of the other terms. The net radiation can also be expressed as an electromagnetic balance of all incoming and outgoing fluxes reaching and leaving a flat horizontal and homogenous surface as:

$$R_n = (1 - \alpha) * R_s + E_a R_l - \epsilon \sigma T_s^4 \quad (7)$$

where α represent surface albedo, R_s is short wave incoming solar radiation ($0.3\text{--}3 \mu\text{m}$), E_a represent atmospheric emissivity, R_l is incoming long wave radiation ($3\text{--}100 \mu\text{m}$), ϵ represent emissivity, σ is Stefan Boltzmann constant and T_s is surface temperature.

The incoming short wave radiation is the portion of the visible energy from the sun and it can be evaluated from remote sensors as,

$$R_s = G_{sc} * \cos \theta * dr * \tau_{sw} \quad (8)$$

where G_{sc} shows solar constant (1367 W/m^2), $\cos \theta$ represent sun elevation angle, dr is inverse square relative earth sun distance, τ_{sw} is represent transmittance.

$$dr \text{ is also calculate using : } dr = 1 + 0.033 \cos \left(\text{Doy} \frac{2\pi}{365} \right) \quad (9)$$

where *Doy* is the Julian day.

$$\tau_{sw} \text{ Transmittance is derived using } \tau_{sw} = 0.75 + 2 * 10^{-5} * z \quad (10)$$

z is the elevation.

The equation of long wave outgoing radiation is,

$$R_l = \sigma T_a^4 \quad (11)$$

σ represents Stefan Boltzmann constant, T_a is ambient air temperature.

The surface albedo is estimated as regression (Liou et al. 2008)

$$\alpha = 1.0488 \tau_{\text{blue}} + 1.1779 \tau_{\text{green}} + 0.31132 \tau_{\text{red}} - 0.65569 \tau_{\text{NIR}} \quad (12)$$

Atmospheric emissivity (E_a) is the efficiency with which the atmosphere emits as compared to black body and is estimated based on the empirical equation (Brutsaert, 1982),

$$E_a = 1.24 \left(\frac{e_a}{T_a} \right)^{1/7} \quad (13)$$

where e_a represent vapor pressure of air and T_a is ambient air temperature.

The vapor pressure of air in contact with its liquid form is estimated as,

$$e_a = P_s * \frac{RH}{100} \quad (14)$$

P_s is saturated vapor pressure and RH is relative humidity.

Saturated vapor pressure is estimated as,

$$P_s = 1013.25 * \exp \left(13.3185 t_r - 1.9760 t_r^2 - 0.6445 t_r^3 - 0.1299 t_r^4 \right) \quad (15)$$

where

$$t = 1 - (373.15/T), \text{ where } T = \text{surface temperature} \quad (16)$$

Ground heat flux (G) can be presented by the amount of heat transmitted per unit area per unit time. Soil heat flux which is determined by the thermal conductivity of soil and temperature gradient of the topsoil is derived using,

$$G = (0.1 - 0.042 h) R_n \quad (17)$$

h is the reference height

The mathematical formulation of the sensible heat flux is based on the theory of mass transport of heat and momentum between the surface and the near surface environment. The expression can be written as,

$$H = \rho C_p \frac{T_s - T_a}{r_a} \quad (18)$$

where ρ is the air density, C_p is specific heat, T_s is surface temperature, T_a is ambient air temperature, r_a is aerodynamic resistance.

T_a is estimated as,

$$T_a = m * z + T_0 \quad (19)$$

where m is the slope between temperature and air, z is soil surface elevation, T_0 is air temperature at sea level.

Aerodynamic resistance (r_a) is the resistance for heat transport between surface and air. It varies with wind speed with intensity and direction of sensible heat itself, and therefore the iterative computation is the only way for its estimation (Brutsaert, 1982),

$$r_a = \frac{\{\ln(z - d)z_0\}^2}{k^2 * U} \quad (20)$$

where z is average height of tree, d represent zero plane displacement height, z_0 is surface roughness height, k is Von karman constant and U is the wind speed (m/s). The Von Karman constant named for Theodore Von Karman, is a dimensionless constant describing the logarithmic velocity profile of a turbulent fluid flow, near a boundary with no slip condition.

Zero plane displacement (d) is the height in meters above the ground at which zero wind speed is achieved as a result of flow obstacles such as tree or building and is described as,

$$d = \frac{2h}{3} \quad (21)$$

where h is height of obstacles

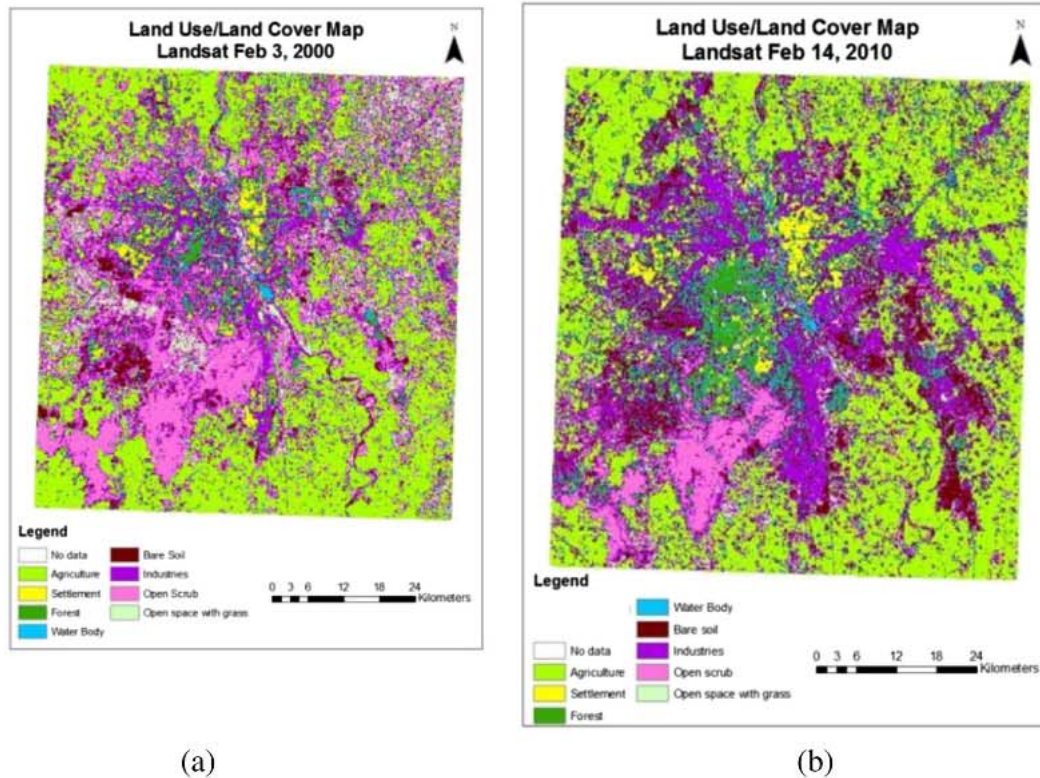


Fig. 1. LU/LC map of Landsat (a) February 3, 2000 and (b) February 14, 2010

Surface roughness height (z_0) commonly parameterize by length scale called roughness length. z_0 is the height where the mean wind speed becomes zero if the wind profile has a logarithmic variation with height and is estimated as,

$$z_0 = \frac{h}{8} \quad (22)$$

The latent heat is estimated as,

$$LE = \rho C_p \frac{e_s - e_a}{\gamma(r_a + r_s)} \quad (23)$$

where γ the psychrometric constant (hPa/K), e_s is the saturation vapor pressure (hPa) at the surface temperature, and r_s is the stomatal resistance (s/m) which depends on vegetation, meteorological and atmospheric conditions.

The sensible heat flux due to radiant heat balance, and expressed as H_n , can be calculated as the residue of the heat balance equation,

$$H_n = R_n - G - LE \quad (24)$$

Finally, the sensible heat flux due to the artificial/anthropogenic (H_{as}) effects is estimated as the difference between the total sensible heat flux and natural sensible heat,

$$H_{as} = H - H_n \quad (25)$$

where H_{as} is the net increase in sensible heat flux from the surface heat balance and is not equivalent to A . When the total H calculated is smaller than H_n , H is substituted for H_n .

5. Results and discussion

5.1. LU/LC analysis using Landsat data

The change in LU/LC over the last 10 year period was studied using Landsat-TM 5 datasets of February 2, 2000 and February 14, 2010 (Fig. 1a and b). The population of Delhi soared to 16.7 million according to census of India 2011 and population density to 11,297 person per sq. km which is highest in the country and has direct impact on the LU/LC changes.

It is evident from Fig. 1, that most of the changes/development is observed in and around south eastern part of Delhi. Over the last 10 years, urban structures like multinational office buildings, multiplexes, shopping malls, apartments and residential have come up in Noida and Greater Noida areas. New developments like shopping malls, apartments and industrial area have been developed in and around north eastern part near Ghaziabad and the same increase in urban structures are also observed in southern part Faridabad and north eastern part of Delhi.

Table 2
Area statistics of different LU/LC from year 2000 to 2010.

Landsat Feb 3, 2000			Landsat Feb 14, 2010		
LU/LC	Area (Km ²)	Area (%)	LU/LC	Area (Km ²)	Area (%)
Agriculture	1954.91	37.89	Agriculture	1884.23	36.52
Settlement	291.93	5.66	Settlement	605.9	11.74
Water body	44.53	0.86	Water body	24.95	0.48
Open scrub	1149.15	22.27	Open scrub	604.08	11.71
Open space with grass	849.68	16.47	Open space with grass	610.50	11.83
Forest	147.70	2.86	Forest	268.51	5.20
Bare soil	468.0	9.07	Bare soil	549.54	10.65
Industrial	254.10	4.92	Industrial	612.29	11.87

The analysis of LU/LC change statistics (Table 2) shows that during the last 10 years, there is marginal change in agricultural, forest, bare soil & water body while substantial change in open scrub, settlement & industrial/commercial which is due to the increasing population and massive urbanization. The India State of Forest Report of year 2001 and 2011 by Forest Survey of India over Delhi reveals that the area under forest in the last one decade has increased by nearly 110%.

5.2. Analysis of land surface temperature

The LST maps for summer and winter seasons of 2000 and 2010 (Landsat and MODIS) clearly show high amplitude of surface temperature in 2010 than in 2000 due to LU/LC changes attributing mainly to increase in urban built-up area (combination of settlement and industrial area) (Figs. 2 and 3). By observing the Landsat derived LST maps of both seasons, it is observed that the maximum

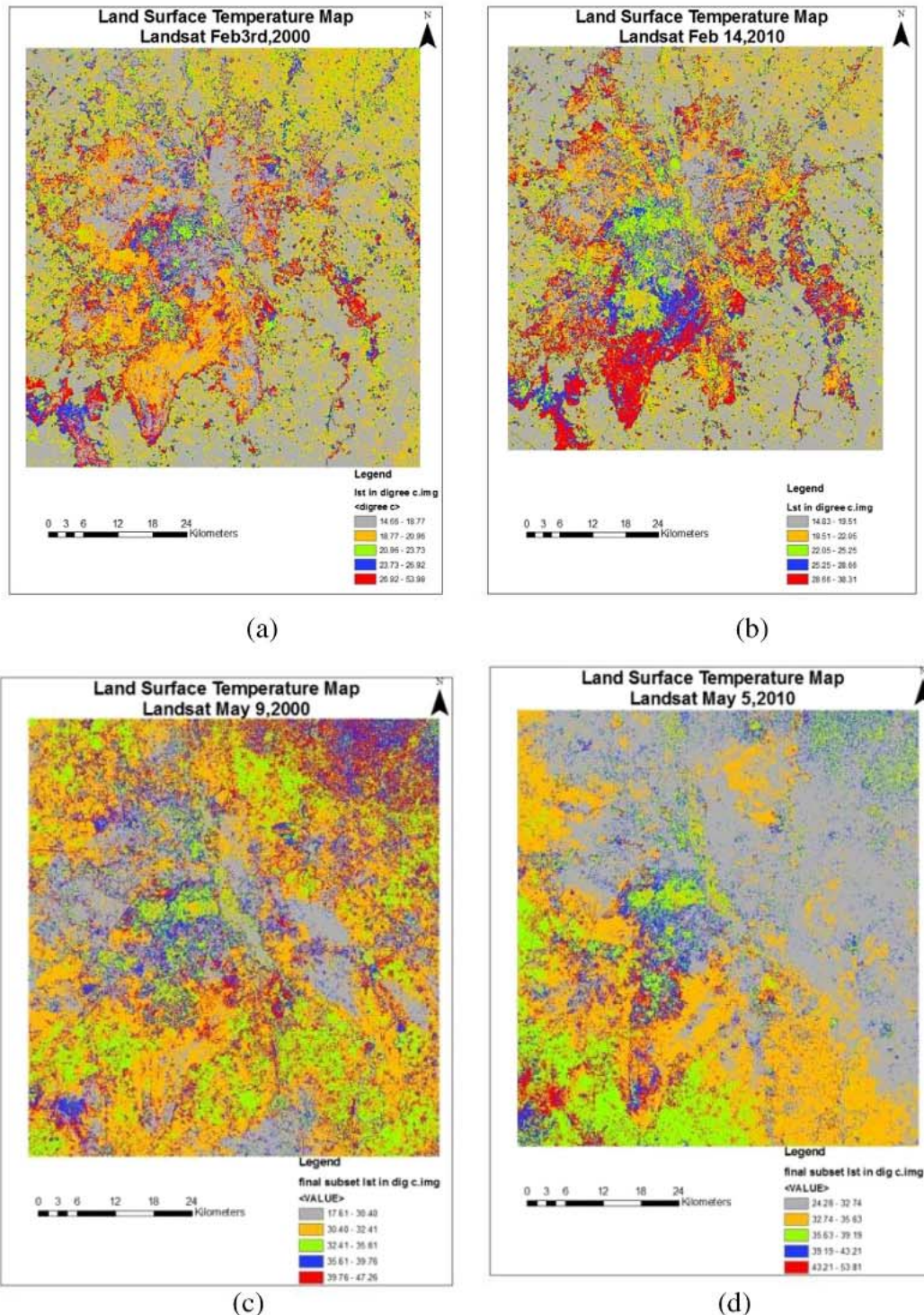


Fig. 2. Land surface temperature images of Landsat data (a) February 3, 2000 (b) February 14, 2010 (c) May 9, 2000 and (d) May5, 2010

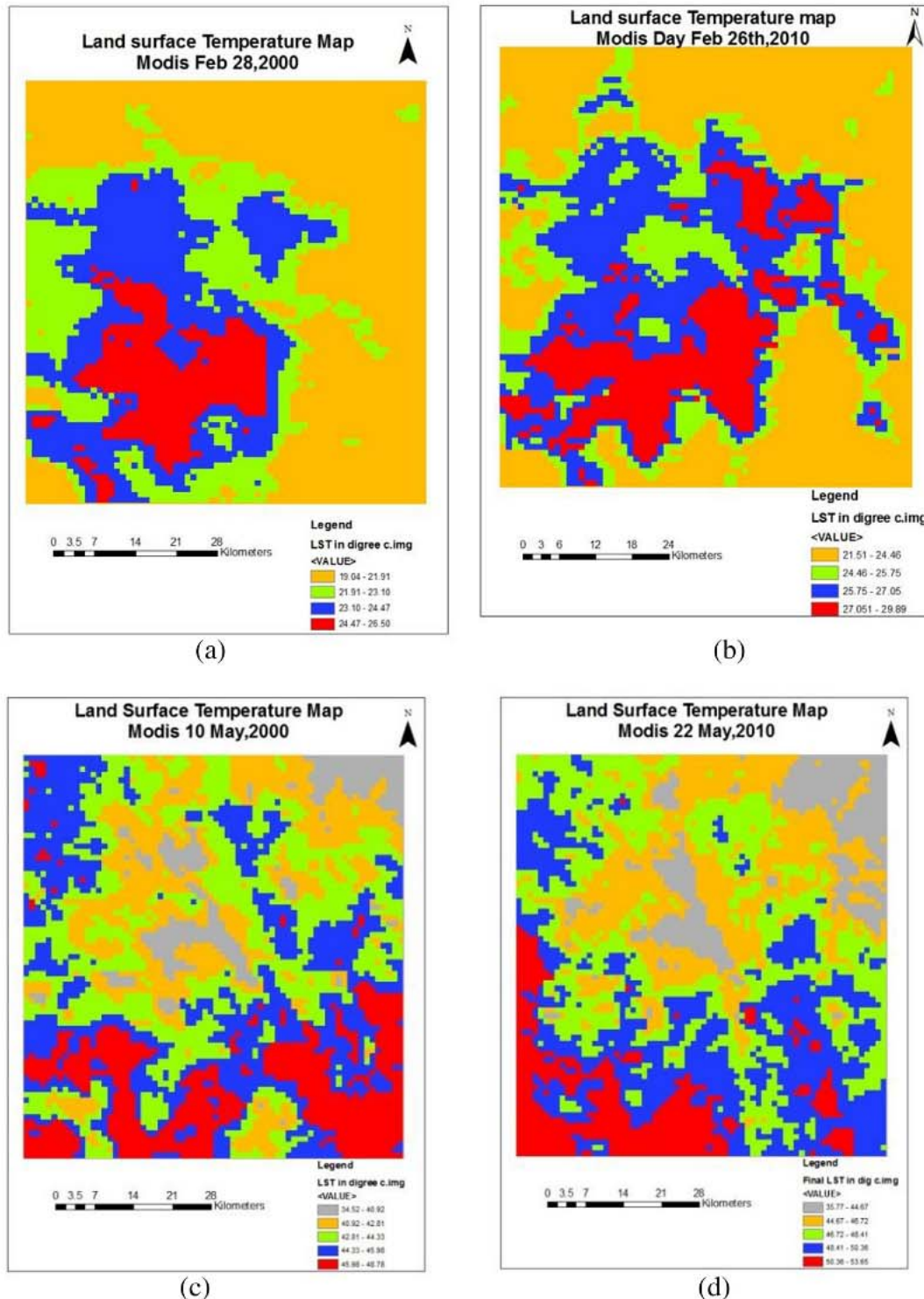


Fig. 3. Land surface temperature image of Modis (a) February 28, 2000 and (b) February 26, 2010 (c) May 10, 2000 and (d) May 22, 2010.

land surface temperature are observed over urban built-up and open space. The surface temperature over industrial and settlement are high in both the months of 2000 and 2010 and that over agricultural land (fallow land) in May is found to be higher than February in all years (due to change to fallow in May). Open space with grass also shows high temperature in May due to same reason. The same trend is followed and observed in Landsat and MODIS datasets. Over Landsat data the temperature gradients are clearly visible while in MODIS the gradients are not fine enough. Table 3

shows the average temperature variations over different LU/LC for both the seasons. In general, the surface temperature in MODIS is observed to be higher than that of Landsat data which is due to its coarser resolution. Over Landsat it is observed that the temperature increase is around ± 2 °C (average increase in winter season over all LU/LC is observed to be around 0.8 °C while during summer is 2.4 °C) while using MODIS is observed around ± 3 °C (average increase in winter season over all LU/LC observed to be around 1.8 °C while during summer is 4.0 °C) during the last 10 years period. It is

Table 3

Comparison of derived LST using satellite data for different months of year 2000 & 2010.

Land use/land cover	Winter season				Summer season			
	Landsat 2000 Feb (°C)	Landsat 2010 Feb (°C)	Modis 2000 Feb (°C)	Modis 2010 Feb (°C)	Landsat 2000 May (°C)	Landsat 2010 May (°C)	Modis 2000 May (°C)	Modis 2010 May (°C)
Industrial	22.2	24.2	25.3	28.3	30.1	32.5	43.8	48.2
Agriculture	17.7	17.6	22.3	23.9	33.2	38.1	44.1	47.1
Open space with grass	21.7	21.4	24.2	25.5	30.1	34.4	41.5	45.5
Settlement	22.3	22.2	23.9	26.4	32.5	33.6	44.0	47.7
Forest	18.6	18.2	23.9	25.2	31.1	29.8	40.3	41.5
Water body	15.3	16.7	22.1	23.7	23.4	24.1	33.2	41.5

inferred that for surface temperature estimation over Delhi, Landsat provides accurate results than MODIS while for regional level studies MODIS data could be a good option.

The comparison of satellite and ground based measured LST was analyzed. The ground data collection and field measurements were only possible during 2010. The comparison of satellite derived LST with that of ground measured values was done over the same GPS locations using thermal infrared thermometer (Table 4). It was observed that Landsat estimated LST values are in close agreement with that of ground measured data within an error of ± 2 °C (compared for the same solar time of satellite pass). The comparison for MODIS estimated LST with ground data is found to be within an error of ± 6.5 °C (compared for the same solar time of satellite pass) due to the fact that the pixels have mixed LU/LC classes and the boundaries are not crisp. In the study the inter-normalization of Landsat and MODIS was not done.

Net radiation was estimated from albedo, surface emissivity, surface and atmospheric temperature and solar radiation. Sensible and latent heat fluxes were estimated via the bulk resistance, wind speed, relative humidity, air emissivity, vapor pressure, air temperature and specific heat. Ground heat flux was estimated using the net radiation and the thermal conductivity of soil. Finally the artificial heat flux for all the seasons was evaluated. The estimated artificial heat flux (H_{as}) during winter season of year 2000 using Landsat showed that the values are in the range of 20.78 to 56.25 W/m² while during 2010 in the range of 17.01–149.36 W/m² (Fig. 4a and b). The estimated artificial heat flux (H_{as}) during summer season of year 2000 and 2010 is found to be in the range of 37.66 to 57.40 W/m² and 49.79 to 220.96 W/m² respectively. As observed, the dynamic range of H_{as} values in year 2010 is increased revealing that there is a strong anthropogenic influence in the rise of artificial heat flux over various LU/LC in the past 10 years

(Table 5). The statistics shows that the H_{as} over the last 10 years has increased almost by 150% over settlement and concrete structures.

The artificial heat flux (H_{as}) is also studied using the MODIS data over winter and summer months (Fig. 5). MODIS February 2000 image shows that the values are in the range of 230.52 to 134.51 W/m² while in 2010 the range is 184.86 to 230.67 W/m². The summer H_{as} values for year 2000 are observed to be in the range of 11.57 to 229.57 W/m² while in 2010 in range of 154.59 to 220.07 W/m². The statistics shows the mean H_{as} over the last 10 years as observed by MODIS data has increased over settlement and concrete structures (Table 6). This is clearly observed in the MODIS image where more area under high H_{as} values (settlement) has increased in the last 10 years. The Artificial heat flux values have been compared with literature (Soushi and Yasushi, 2005) over all features and are found comparable.

6. Conclusion

The research has been undertaken to evaluate the potential of satellite data in studying the spatial, temporal and seasonal variation of surface temperature, natural and anthropogenic heat fluxes & associated bio-physical parameters and analyze the influence of LU/LC on heat distribution over Delhi and surrounding areas. It is observed at the city level, LU/LC has profound influence on surface temperature and heat fluxes regime. High temperature zones have been observed over bare soil, open scrub, industrial and built-up. High surface temperature is attributing mainly due to low amount of vegetation. From the analysis, it is inferred that over the span of ten years (2000–2010), there is increase of ± 2 °C as observed by Landsat and ± 7.0 °C as observed by MODIS data in the mean surface temperature over built-up areas. The influence of land use/land cover on surface temperature and anthropogenic heat fluxes was analyzed. During the period of 10 years, overall the increase in mean surface temperature was observed due to changes in various LU/LC while few areas showed decrease in surface temperature. The increase in surface temperature at city level mainly attributed due to cumulative impact of all changes in LU/LC, increase in population amount of vegetation. Anthropogenic heat fluxes over settlement using February 2000 and 2010 of Landsat image showed 12.47 W/m² and 31.26 W/m² respectively while anthropogenic heat fluxes using February 2000 and 2010 of MODIS image showed 92.16 W/m² and 132.80 W/m² respectively. The same trend is depicted in May month images of both datasets. Coarser resolution satellite dataset (MODIS) did not give much information of the surface temperature and heat fluxes related to heterogeneous and complex built up areas. Hence, thermal remote sensing (with high spatial resolution) is one viable option to help in realistic assessment of surface temperature and heat fluxes of built up areas. It is true that the MODIS data did not show optimistic results but for larger regions and with high temporal resolution, MODIS data could be useful. Anthropogenic heat flux (H_{as}) can be considered as an indicator of the strength of urban heat island

Table 4

Comparison of LST derived using different satellite & ground measured data.

Land use/land cover	Date & time (ground data)	Ground temp ^a (°C)	Landsat 2010 May (°C)	Modis 2010 May (°C)
Industrial	22/5/2010 10:47 am	39.9	38.0	44.1
Settlement	22/5/2010 12:45 pm	34.1	32.7	43.5
Agriculture	23/5/2010 4:30 am	35.1	31.8	38.2
Open space with grass	23/5/2010 10:18 am	36.1	35.4	41.5
Settlement	24/5/2010 12:15 pm	34.2	33.2	43.7
Industrial	24/5/2010 10:30 am	34.5	37.0	46.0
Road side built up	25/5/2010 12:30 pm	36.2	39.1	41.1
Open space with grass	25/5/2010 12:45 pm	36.7	35.4	42.5

^a Average values of at least 10–15 measured samples.

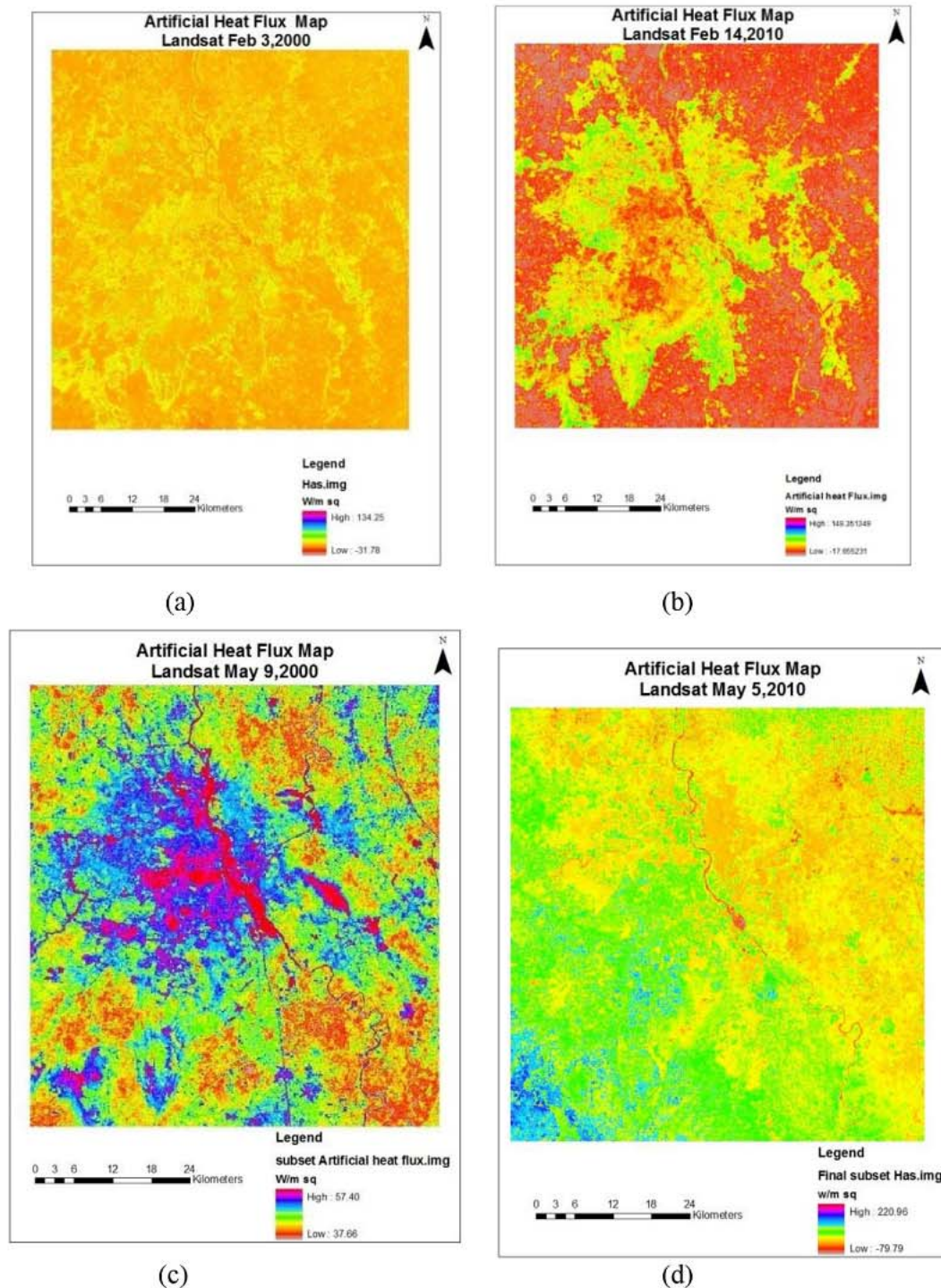


Fig. 4. Artificial heat flux images over Delhi and surroundings (a) Landsat Feb 3, 2000, (b) Landsat Feb 14, 2010, (c) May 9, 2000 and (d) May 5, 2010.

effect, and can be used to quantify the magnitude of the urban heat island effect in the future. In future analysis, H_{as} can be estimated with higher accuracy by using a more detailed parameterization particularly on the ground and latent heat fluxes.

7. Implications on planning—managing the urban heat

An examination of the linkage between urban development, the ground based measurements, satellite derived land surface temperatures and heat fluxes provides a theoretical model of the

dynamics of an urban thermal environment which is useful for urban planning and decision making. Many studies have reported widely and successfully applied measures on mitigating the urban heat island effects with promising financial and environmental benefits.

Based on the results of this study, the following planning implications can be derived:

- It is seen that almost all anthropogenic heat enters into the environment instantly and directly while only part of solar

Table 5

The Artificial heat flux over different LU/LC using Landsat data for winter and summer season.

Land use/land cover	Winter		Summer	
	Feb (2000) W/m ²	Feb (2010) W/m ²	May (2000) W/m ²	May (2010) W/m ²
Water body	−13.40	−4.79	36.83	−13.75
Forest	−5.03	−9.86	39.82	31.95
Agriculture	−3.7	−9.09	40.86	80.10
Settlement	12.47	31.26	66.73	120.39
Open scrub	12.12	36.32	47.05	97.32
Bare soil	16.12	54.79	49.18	116.63

radiations heats up the environment directly, the rest are absorbed by the complicated urban built structures and heat up the environment indirectly. The basic heat transfer and energy conservation processes, such as conduction, convection and radiation play their characteristic roles in this heat exchange. The method and quantity of heat released by the urban structures, however, depends on other controllable factors such as the sky view factor and building material (Memon et al., 2008).

- Urban heat island (UHI) effect is increased due to continuous increasing of urban buildings which is due to increases of urban structures like multinational office buildings, multiplexes,

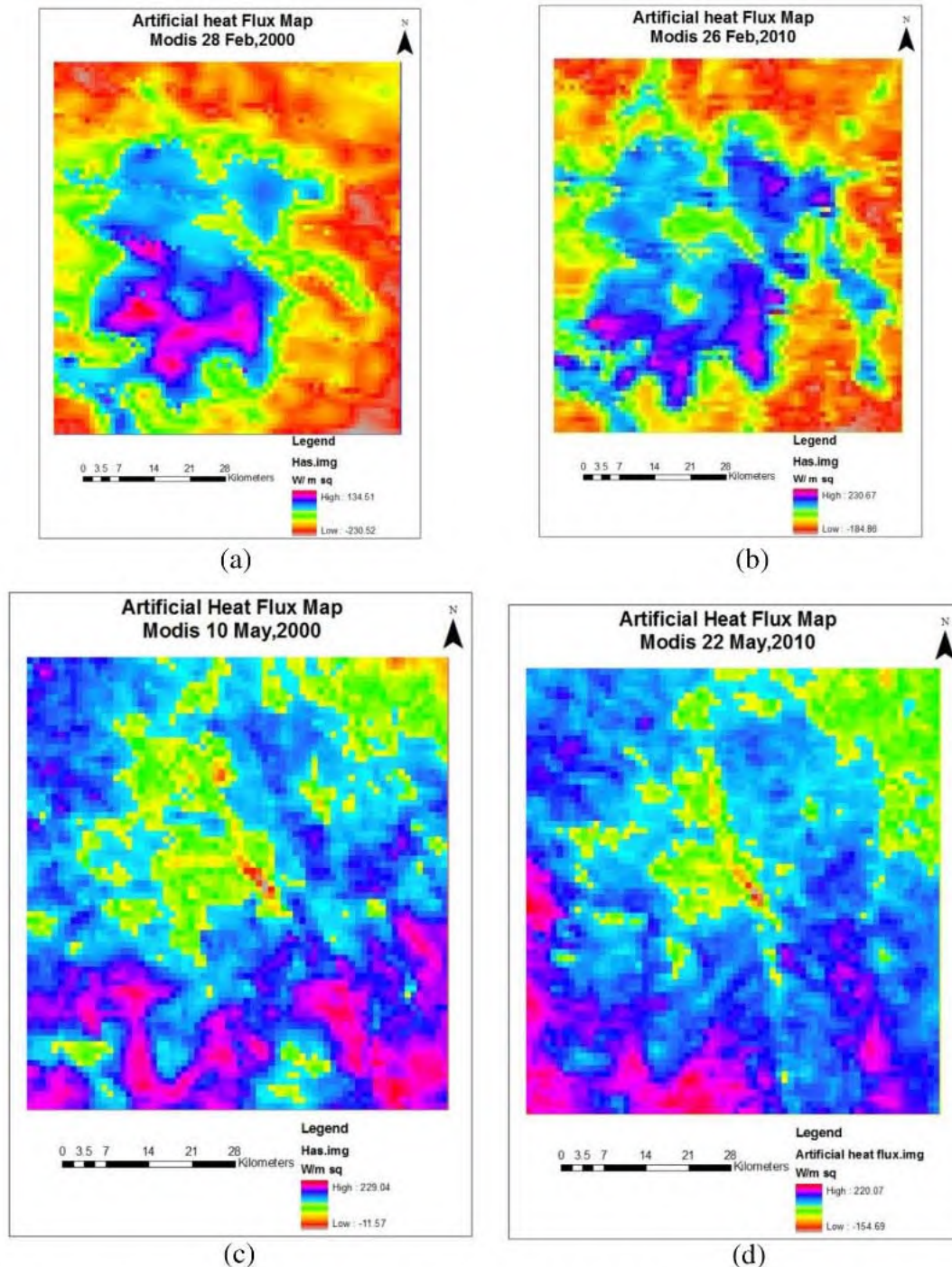


Fig. 5. Artificial heat Flux images over Delhi and surroundings (a) Modis February 28, 2000 (b) Modis February 26, 2010, (c) May 10, 2000 and (d) May 22, 2010.

Table 6
The Artificial heat flux over different LU/LC using MODIS data for winter and summer season.

Land use/land cover	Winter		Summer	
	Feb (2000) W/m ²	Feb (2010) W/m ²	May (2000) W/m ²	May (2010) W/m ²
Water body	−108.29	−68.22	−11.57	−79.75
Forest	−133.91	−56.21	13.81	61.95
Agriculture	−200.32	−180.64	43.78	62.10
Settlement	92.16	132.80	158.01	217.77
Open scrub	45.07	93.99	143.21	201.14
Bare soil	80.91	119.12	144.22	200.40

shopping malls, apartments and residential areas. It can be attributed in the study that a change of 5% change in LST increases sensible heat flux by around 3% while anthropogenic heat flux by 2%. It is also believed that the albedo is very low in cities due to typical street canyon configurations and is one of the main reasons of high air and surface temperatures. In the current study, the albedo change (decrease) over urban areas during summer and winter season was observed to be around 11% and 9% thereby attributing the changes in H_{as} by around 7% and 6% respectively.

- Due to the lack of vegetation, cities exhibit little latent heat of vaporization while high roughness of structures in urban areas reduces the amount of convective heat removal and transfer by wind. Many studies have established that UHI is negatively correlated with wind speed and cloud cover while positively correlated with the city population. From the study it is inferred that during the last 10 year period, the land use area under settlement including industrial and Forest increased by 13.0 and 2.3% respectively while decrease in land cover like open scrub, open spaces and water by 10.5, 4.6 and 0.38% respectively. There is also an unprecedented increase of around 21.6% increase in city population (Census, 2011) enabling high energy consumption, heat dissipation causing high surface temperatures and ultimately enhancing anthropogenic heat flux. In the absence of increase of land cover under forest and parks, the estimated anthropogenic heat flux increase would have been up by another 12%.
- The Government of Delhi initiated plantations in coordination with concerned agencies along railway lines, railway stations, along the drains, village community lands and villages, bunds of agricultural lands, farm lands etc. Initiatives such as free distribution of saplings through 13 departmental nurseries and through the nurseries of other greening agencies were also undertaken. Novel approaches such as free distribution of saplings through petrol pumps and Mother Dairy milk vending booths during monsoon season yielded productive results which helped the forest area to increase from 2.85 to 5.20%. But still it's not enough as compared to the increasing rate of urbanization.
- Inputting and mitigating upwelling thermal energy into the atmosphere varies over different types of vegetation. The area with trees are cooler (low temperature) than grass lawns and parks. Hence, maintaining and enhancing urban forest gives a hopeful solution of maintaining urban heat. City planners and government should concentrate more on green campaigns.
- It is easily understandable from satellite imagery that tree lines roads, water bodies, parks and garden show low temperatures. Hence, it is important to increase road side trees and also gardens/parks in the city. As well as Yamuna river need to be cleaned as it is contaminated due to anthropogenic and

industrial waste causing water pollution and indirectly increases the temperature.

- It is observed that densely and unplanned urban areas shows intense increase in anthropogenic heat flux. Hence, by segregating, planned, open, airy spaces and unplanned dense urban areas helps in understanding the spatial pattern of the anthropogenic heat flux.
- From the study we can widely and successfully apply measures on mitigating the urban heat island effects with hopeful financial and environmental benefits. The possible mitigating UHI effects could broadly be related to reducing anthropogenic heat release e.g. effective use of air conditioners and other electric appliances and related to better roof design. Reducing anthropogenic heat and energy consumption improvement in building designs will help to improve urban environment.
- Green buildings technology across all its major construction agencies and municipality through a circular issued in year 2003 by the Government of Delhi had decided to be adopted. The green building concept emphasizes sustainable site planning, design and construction of buildings to achieve maximum harmony with nature and at the same time reduces negative environmental effects.
- For understanding thermal response of each LU/LC types and the thermal effect of spatial arrangement of different LU/LC types, satellite imagery can be used to derive information on LU/LC types and surface temperature at high spatial and temporal resolutions.

References

- Boegh, E., Soegaard, H., 2004. Remote sensing based estimation of evapotranspiration rates. *Int. J. Remote Sens.* 25 (3), 2535–2551.
- Brutsaert, W., 1982. *Evaporation into the Atmosphere: Theory, History and Applications*. D. Reidel Publishing Company, p. 299.
- Carlson, T.N., 1986. Regional-scale estimates of surface moisture availability and thermal inertia using remote thermal measurements. *Remote Sens. Rev.* 1, 197–247.
- Chang, Tzu-Yin, Liou, Yuei-An, Lin, Chuan-Yao, Liu, Shaw-Chen, Wang, Yi-Chen, 2010. Evaluation of surface heat fluxes in Chiayi plain of Taiwan by remotely sensed data. *Int. J. Remote Sens.* 31 (14), 3885–3898.
- Dousset, B., Gourmelon, F., 2003. Satellite multi-sensor data analysis of urban surface temperatures and land cover. *ISPRS J. Photogramm. Remote Sens.* 58, 43–54.
- Grind, Van de, Owe, M., 1993. On the relationship between thermal emissivity & NDVI for natural surface. *Int. J. Remote Sens.* 14, 1119–1131.
- Kant, Y., Badrinath, K.V.S., 2002. Ground based method for measuring thermal infrared effective emissivity: implication and perspective on the measurement of land surface temperature from satellite data. *Int. J. Remote Sens.* 23 (11), 2179–2191.
- Liou, Y.-A., Chang, T.-Y., Ho, H.-J., 2008. Estimation of evapotranspiration by using Modis imagery over Chiayi Plain in Taiwan. In: *Cross-strait Symposium on the Remote Sensing Work Shop*, 15–19 September 2008, Guilin China. Institute of Remote Sensing Application, Chinese Academy of Science, Beijing, China, pp. 100–110.
- Mansor, S.B., Cracknell, A.P., 1994. Monitoring of coal fire using thermal infrared data. *Int. J. Remote Sens.* 15 (8), 1675–1685.
- Memon, R.A., Leung, D.Y.C., Chucho, L., 2008. A review on the generation, determination and mitigation of urban heat island. *J. Environ. Sci.* 20, 120128.
- NASA, 2004. *Landsat Project Science Office: Landsat 7 Science Data Users Hand Book*. Chapter: 11, Data Products <http://www.gsfc.nasa.gov/las/handbook/handbook.html>.
- Nichol, J., 1995. Monitoring tropical rain forest microclimate. *Photogram. Eng. Remote Sens.* 61 (9), 1159–1165.
- Rubio, E., Caselles, V., Badenas, C., 1997. Emissivity measurements of several soils and vegetation types in the 8–14 μ m waveband: analysis of two field methods. *Remote Sens. Environ.* 59, 490–521.
- Soushi, Kato, Yasushi, Yamaguchi, 2005. Analysis of urban heat-island effect using ASTER and ETM+ data: separation of anthropogenic heat discharge and natural heat radiation from sensible heat flux. *Remote Sens. Environ.* 99, 44–54.
- Srivastava, P.K., Majumdar, T.J., Bhattacharya, A.K., 2010. *Study of Land Surface Temperature and Spectral Emissivity using multi-sensor Satellite Data*. Indian Academy of Science, pp. 67–74.
- Wan, Z., Dozier, T., 1996. A generalized split window algorithm for retrieving land surface temperature from Space. *IEEE Trans. Geosci. Remote Sens.* 34 (4), 892–905.